ACS OMEGA

Open Access



http://pubs.acs.org/journal/acsodf

Article

# Synthesis and Biological Activity of 2-Chloro-8-methoxy-5-methyl-5*H*-indolo [2,3-*b*] Quinoline for the Treatment of Colorectal Cancer by Modulating PI3K/AKT/mTOR Pathways

Yunhao Ma,[§] Hongmei Zhu,[§] Xinrong Jiang, Zhongkun Zhou, Yong Zhou, Yanan Tian, Lixue Tu, Juan Lu, Yuqing Niu, Liqian Du, Zhenzhen Si, Hong Fang, Huanxiang Liu, Yingqian Liu,* and Peng Chen*

Cite This: *ACS Omega* 2024, 9, 30698−30707

Read Online

ACCESS | Metrics & More | Article Recommendations | Supporting Information

**ABSTRACT:** Developing novel drugs from natural products has proven to be a very effective strategy. Neocryptolepine was isolated from *Cryptolepis sanguinolenta*, a traditional endemic African herb, which exerts a wide range of biological activities such as antimalaria, antibacterial, and antitumor. 2-Chloro-8-methoxy-5-methyl-5*H*-indolo [2,3-*b*] quinoline (compound **49**) was synthesized, and its cytotoxicity was assessed on pancreatic cancer PANC-1 cells, colorectal cancer HCT116 cells, liver cancer SMMC-7721 cells, and gastric cancer AGS cells *in vitro*. The results of the *in vitro* assay showed that compound **49** exerted remarkable cytotoxicity on colorectal cancer HCT116 and Caco-2 cells. The cytotoxicity of compound **49** to colorectal cancer HCT116 cells was 17 times higher than that of neocryptolepine and to human normal intestinal epithelial HIEC cells was significantly reduced. Compound **49** exhibited significant cytotoxicity against the colorectal cancer HCT116 and Caco-2 cells, with $IC_{50}$ of 0.35 and 0.54 $\mu$M, respectively. The mechanism of cytotoxicity of compound **49** to colorectal cancer HCT116 and Caco-2 cells was further investigated. The results showed that compound **49** could inhibit colony formation and cell migration. Moreover, compound **49** could arrest the cell cycle at the G2/M phase, promote the production of reactive oxygen species, reduce mitochondrial membrane potential, and induce apoptosis. The results of Western blot indicated that compound **49** showed cytotoxicity on HCT116 and Caco-2 cells by modulating the PI3K/AKT/mTOR signaling pathway. In conclusion, these results suggested that compound **49** may be a potentially promising lead compound for the treatment of colorectal cancer.

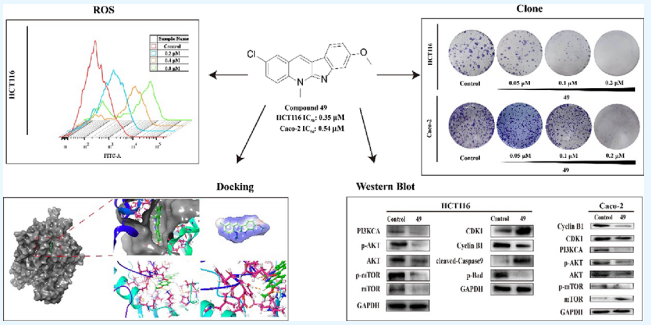


## 1. INTRODUCTION

Colorectal cancer (CRC) is a highly aggressive and common malignancy in the world.[1−3] Global cancer statistics for 2020 showed that there are approximately 1.93 million new cases of colorectal cancer and approximately 0.93 million colorectal cancer deaths worldwide, ranking third in incidence and second in mortality of all malignancies.[4] Currently, the main treatments for CRC include surgery, chemotherapy, radiotherapy, immunotherapy, and targeted therapies.[5−7] Chemotherapy remains the most commonly used treatment method in clinical.[8] At present, the commonly used chemotherapy drugs mainly include 5-fluorouracil (5-Fu), oxaliplatin, irinotecan, capecitabine, and so on. Combination therapy strategies are widely used in clinical treatment.[9] Although chemotherapy has improved the survival rate of patients with colorectal cancer, its disadvantages, such as high toxicity and side effects, easy to produce drug resistance, and so on, cannot be ignored,[10,11] Therefore, it is necessary to develop novel high-efficiency and low-toxic chemotherapy drugs against colorectal cancer.[12]

Natural products are considered a promising source for novel anticancer drugs.[13,14] The analysis of anticancer drugs showed that most of the approved drugs are unmodified natural products or semisynthetic derivatives, or molecules synthesized based on the pharmacophores of natural product compounds.[15−17] It has been reported that the indole quinoline alkaloids have good antibacterial and antitumor activities.[18,19] Neocryptolepine is a promising alkaloid isolated from the traditional endemic African herb *Cryptolepis sanguinolenta*, whose broad bioactivity including cytotoxicity,

**Received:** April 1, 2024
**Revised:** June 12, 2024
**Accepted:** June 19, 2024
**Published:** July 2, 2024

**Scheme 1. Synthetic Route of Compound 49**[a]

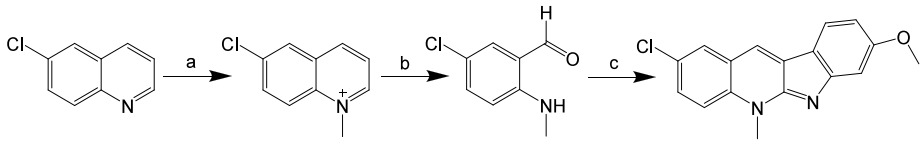


[a]Reagents and conditions: (a) IPA, $CH_3I$, 3 h; (b) KOH, $H_2O_2$, 48 h; (c) 6-methoxyindole, *p*-TSA, EtOH, 24 h.

antibacterial, antifungal, and antiplasmodial has been confirmed by several studies.[20,21] Also, structural modification of compounds is an effective method to enhance pharmacological activity.[22,23] Therefore, it is valuable to design and evaluate the cytotoxic activity of a neocryptolepine derivative against colorectal cancer cells.

The occurrence and development of colorectal cancer are related to a variety of signal transduction pathways.[24] The PI3K (phosphatidylinositol 3-kinase)/AKT (protein kinase B)/mTOR (mammalian target of rapamycin) signaling pathway is one of the most commonly abnormally activated signaling pathways in colorectal cancer.[25] This signaling pathway can regulate the vital activities of cancer cells such as autophagy, proliferation, apoptosis, drug resistance, and metastasis.[26] Studies have been done to develop drugs that target the significant protein of the PI3K/AKT/mTOR signaling pathway; a number of drugs have been evaluated in clinical trials, and it is becoming increasingly clear that inhibitors of PI3K/AKT/mTOR can effectively inhibit tumor progression.[27,28] However, few inhibitor drugs have been approved for clinical use, and those that have been approved for clinical use are mainly PI3K and mTOR inhibitors. The modulation of the PI3K/AKT/mTOR signaling pathway may be a good strategy for the treatment of colorectal cancer.

In the present study, attracted by rational drug design, 2-chloro-8-methoxy-5-methyl-5*H*-indolo [2,3-*b*] quinoline (compound **49**) was designed and synthesized based on the core structure of neocryptolepine. We performed cytotoxicity evaluation on several cell lines and found that compound **49** showed better cytotoxicity on colorectal cancer HCT116 and Caco-2 cells. Subsequently, the potential cytotoxic mechanism of compound **49** was studied. This work may lay the foundation for further structural modification of compound **49** and its development into a promising clinical anticancer drug.

## 2. MATERIALS AND METHODS

**2.1. Synthesis.** All of the reagents and solvents used in the synthesis of compound **49** were commercially purchased from suppliers and used directly without further purification. The synthetic route of compound **49** is outlined in Scheme 1. The synthesized compound **49** was characterized by $^{13}C$ NMR, $^{1}H$ NMR, mass spectrometry, and purity analysis (Supporting Information). $^{1}H$ and $^{13}C$ NMR spectra were recorded at 400 and 100 MHz on a Bruker AM-400 and referenced to the solvent signals. Mass spectrometry was recorded using a Bruker Daltonics APEXII49 spectrometer.

**2.2. Cell Culture.** The human colorectal cancer HCT116 cells, pancreatic cancer PANC-1 cells, and gastric cancer AGS cells were purchased from the American Type Culture Collection (HCT116, LOT:70019042, PANC-1, LOT:70018880, AGS, LOT:70012225). Human liver cancer SMMC-7721 cells, human normal intestinal epithelial HIEC cells, and human colorectal cancer SW480 and Caco-2 cells were stored in our own laboratory. HCT116, SMMC-7721, Caco-2, and AGS cells were cultured in RPMI-1640 medium containing 10% fetal bovine serum and 1% penicillin-streptomycin solution. SW480, HIEC, and PANC-1 cells were incubated in Dulbecco's modified Eagle's medium containing 10% fetal bovine serum and 1% penicillin-streptomycin solution. All cell lines were maintained in a humidified atmosphere at 37 °C with 5% $CO_2$.

**2.3. MTT Assay.** When cells were in the logarithmic phase, $1 \times 10^4$ cells/well (100 $\mu$L) were incubated in 96-well plates. The plate was incubated overnight at 37 °C; after exposure of compound **49** (0.1, 0.2, 0.4, 0.6, 0.8, and 1.0 $\mu$M) (for 0, 24, 48, and 72 h), 10 $\mu$L of MTT solution (5 mg/mL MTT in PBS, pH 7.2) was added in plates for 48 h at 37 °C. Then, the reagent was removed, and 100 $\mu$L of DMSO was added to each well. The absorbance of the wells was measured using a microplate reader at 490 nm. The viability of cells was calculated by the formula = 100% × (sample absorbance)/(control absorbance).

**2.4. Migration Assay.** HCT116 cells ($1 \times 10^5$) were seeded in a serum-free medium into the upper chamber, and the nether chamber was filled with 500 $\mu$L of complete cell culture medium with 20% fetal bovine serum. After the incubation of 48 h at the atmosphere of 37 °C and 5% $CO_2$, the HCT116 cells were fixed with 4% (w/v) paraformaldehyde for 40 min. Then, the cells were stained with 1% crystal violet for another 15 min. After being washed with PBS, the numbers of HCT116 cells were observed and counted with ImageJ.

**2.5. Analysis of Cell Cycle Arrest.** The HCT116 and Caco-2 cells were treated with compound **49** in the different concentrations (0.2 and 0.4 $\mu$M) for 24 h. Cells ($1 \times 10^6$) were fixed 75% ethanol overnight. Then, the HCT116 and Caco-2 cells were slowly washed with PBS and incubated with 100 $\mu$L of RNase A about 30 min at 37 °C. PI (400 $\mu$L) was used for staining at 4 °C for 30 min. The cellular distribution was measured by using a flow cytometer (BD Biosciences, USA).

**2.6. Hoechst 33258 Staining.** Sterile round cover slides (12 mm) were placed in 24-well plate, and $1.5 \times 10^5$ HCT116 cells were seeded on the slide and incubated for 24 h. Then, the HCT116 cells were exposed to different concentrations of compound **49** (0, 0.2, 0.4, and 0.8 $\mu$M) for 48 h. The HCT116 cells were stained with Hoechst 33258 dye (10 $\mu$g/mL) (C0021, Solarbio) for about 20 min. Finally, the circular cover slide with HCT116 cells was placed on the slide, and three fields of view were randomly selected for observation and photography (20×) with a Nikon-ECLIPSE 80i fluorescence microscope.

**2.7. Analysis of Cell Apoptosis.** HCT116 and Caco-2 cells of $8 \times 10^5$ cells per well were plated in a 6-well plate before different concentrations of compound **49** (0, 0.2, 0.4, and 0.8 $\mu$M) were added for 48 h. Then, the HCT116 and Caco-2 cells were harvested with trypsin without EDTA. Annexin V/Alexa Fluor 488 staining solution (5 $\mu$L) were added to the cells and incubated for 5 min at room


https://doi.org/10.1021/acsomega.4c03101
ACS Omega 2024, 9, 30698−30707

temperature in the dark. Then, 10 μL of PI staining solution and 400 μL of PBS were added for analysis by flow cytometry (BD Biosciences, USA) and FlowJo V10.

**2.8. Plate Clone Formation Assay.** For plate clone formation assays, HCT116 and Caco-2 cells (500 cells/well) were seeded in 24-well plates. After attachment, cells were treated with compound **49** of various concentrations (0, 0.05, 0.1, and 0.2 μM) for 7 days at the cultured condition. Then, cells were fixed by 4% (w/v) paraformaldehyde for 2 h and stained with 0.1% crystal violet dye solution for 40 min at room temperature, and the cells were washed twice with PBS and observed.

**2.9. JC-10 Staining Analysis.** When cells were in the logarithmic phase, $8 \times 10^5$ HCT116 and Caco-2 cells/well were inoculated in 6-well plates for 24 h, exposed to indicated concentrations of compound **49** (0, 0.2, 0.4, and 0.8 μM). After incubation for 48 h, cells were harvested and washed with PBS twice. Next, JC-10 staining dye solution was added and the HCT116 and Caco-2 cells were rinsed with JC-10 binding buffer. Measurements were performed by flow cytometry (BD Biosciences, USA). FACS data were processed using the FlowJo V10.

**2.10. ROS Assay.** HCT116 and Caco-2 cells of $8 \times 10^5$ cells/well were seeded in a 6-well plate for 24 h. After attachment, cells were treated with compound **49** (0, 0.2, 0.4, and 0.8 μM) for 48 h. Then, the cells were harvested by trypsin without EDTA and washed twice with PBS. After cells were stained with DCFH-DA staining dye solution for 30 min, the fluorescence of DCF was detected by a flow cytometer (BD Biosciences, USA). FACS data were processed using the FlowJo V10.

**2.11. Molecular Docking.** To find the target of compound **49** exerting cytotoxicity to colorectal cancer cells, molecular docking was performed by Schrödinger 10.1. The protein crystal structure of PI3KCA (PDB:6JVF) was obtained from the Protein Data Bank. First, the complex structure was treated, removing crystal water, side chains, and hydrogen atoms from the protein structure and minimizing the energy of the entire structure. Then, compound **49** and protein PI3KCA were docked and the center of binding between small molecules and proteins was used as the docking site of compound **49** in the process, thus completing the whole docking process.

**2.12. Western Blot.** HCT116 cells ($8 \times 10^5$) and Caco-2 cells/well were inoculated in 6-well plates for 24 h. After attachment, cells were treated with compound **49** of 0.4 μM. Then, HCT116 and Caco-2 cells were harvested and lysed in RIPA lysis buffer mixed with protease inhibitor buffer on ice for 30 min. Total protein (25 μg) was resolved by SDS−PAGE and transferred on the polyvinylidene difluoride (PVDF) membrane before blocking by 5% dry nonfat milk in tris-buffered saline plus 0.1% tween for 2 h at room temperature and probing by primary antibody overnight at 4 °C. Then, the membrane was washed with Tris-Buffered Saline Tween (TBST) three times and incubated with the secondary HRP-conjugated antibody for another 1 h at room temperature. Then, the membrane was washed with TBST and scanned using the BCL luminescence system for the protein and Tanon imaging system, and the protein levels were analyzed with ImageJ. All antibodies were purchased from Bioss at a dilute concentration of 1:2000 for primary antibody and 1:10,000 for secondary antibody. All experiments were performed three times. $p$ <0.05 was considered significant.

**2.13. Statistical Analysis.** All the results and statistical analyses were showed by mean ± standard deviation, and the data were analyzed by IBM SPSS statistical software. The differences of analysis components were analyzed by Student's $t$ test ($t$ test), and $p$ <0.05 indicated statistically significant differences between two groups.

## 3. RESULTS AND DISCUSSION

**3.1. Synthesis and Structure Identification of Compound 49.** The compound **49** was obtained under the mild conditions by the work of Vecchione et al.[29] The 6-chlor-1-methylquinolinium iodide was obtained by methylation with 6-chloroquinoline, IPA, and $CH_3I$ for 4 h. Then, 2-(methylamino)-5-chlor-benzaldehyde was synthesized by oxidation with the 6-chlor-1-methylquinolinium iodide and $H_2O_2$ in KOH for 48 h. Finally, 2-(methylamino)-5-chlor-benzaldehyde was cyclized with 6-methoxyindole and $p$-TSA for 24 h to obtain compound **49**. The structure of compound **49** was confirmed by $^1$H NMR, $^{13}$C NMR, and mass spectrometry (Supporting Information, Figures S1−S3). The purity of compound **49** was above 99% by high-performance liquid chromatography (HPLC), and the results are shown in Figure S4, with methanol: acetonitrile = 80:20 as a mobile phase for 30 min. Physical properties of compound **49**: yield, 62%; red solid, mp 180.11−181.23 °C; $^1$H NMR (400 MHz, DMSO-$d_6$) $\delta$ 8.58 (s, 1H), 8.08 (s, 1H), 7.91 (d, $J$ = 6.0 Hz, 1H), 7.88 (d, $J$ = 8.9 Hz, 1H), 7.72 (d, $J$ = 9.1 Hz, 1H), 7.07 (s, 1H), 6.71 (d, $J$ = 8.4 Hz, 1H), 4.20 (s, 3H), 3.81 (s, 3H). $^{13}$C NMR (100 MHz, DMSO-$d_6$) $\delta$ 161.88, 158.05, 156.16, 134.95, 129.92, 128.47, 126.36, 125.64, 122.85, 122.15, 117.45, 116.39, 108.01, 102.83, 55.82, 32.87. MS-ESI $m/z$: calcd for $C_{17}H_{13}ClN_2O$ $[M + H]^+$ 297.0789; found: 297.0791.

**3.2. Cytotoxic and Structure−Activity Relationship Analysis of Compound 49.** The cytotoxicity of compound **49** was evaluated against cancer cell lines and human normal intestinal epithelial HIEC cell. The $IC_{50}$ values of compound **49** are shown in Table 1 on different cell lines for 48 h. Compound **49** exhibited good and selective cytotoxicity on CRC cell lines, especially HCT116 and Caco-2 cells.

**Table 1. Antiproliferative Properties for Compound 49 on Different Cell Lines for 48 h**

| | $IC_{50}$ (μM) | |
|---|---|---|
| cell lines | compound **49** | neocryptolepine |
| HCT116 | 0.35 ± 0.04 | 6.26 ± 1.22 |
| Caco-2 | 0.54 ± 0.04 | 13.54 ± 0.83 |
| AGS | 26.9 ± 0.00 | 5.81 ± 1.91 |
| PANC-1 | >50 | >50 |
| SMMC-7721 | 22.92 ± 2.16 | 19.31 ± 2.71 |
| HIEC | >50 | 31.37 ± 0.44 |

According to Figure 1A, compound **49** exerted cytotoxicity on HCT116 cells in a time-dependent and concentration-dependent manner. The $IC_{50}$ of compound **49** against Caco-2 cells was 0.54 μM, and compound **49** showed better cytotoxic activity than 5-Fu on Caco-2 cells (Figure 1B). For comparison, the $IC_{50}$ values of neocryptolepine on HCT116 cells and human normal intestinal epithelial HIEC cells were 6.26 and 31.37 μM (Figure 1C). The $IC_{50}$ of compound **49** against HCT116 cells was 0.35 μM, while 5-Fu, a CRC chemotherapy drug commonly used in the clinic, had little


https://doi.org/10.1021/acsomega.4c03101
ACS Omega 2024, 9, 30698−30707

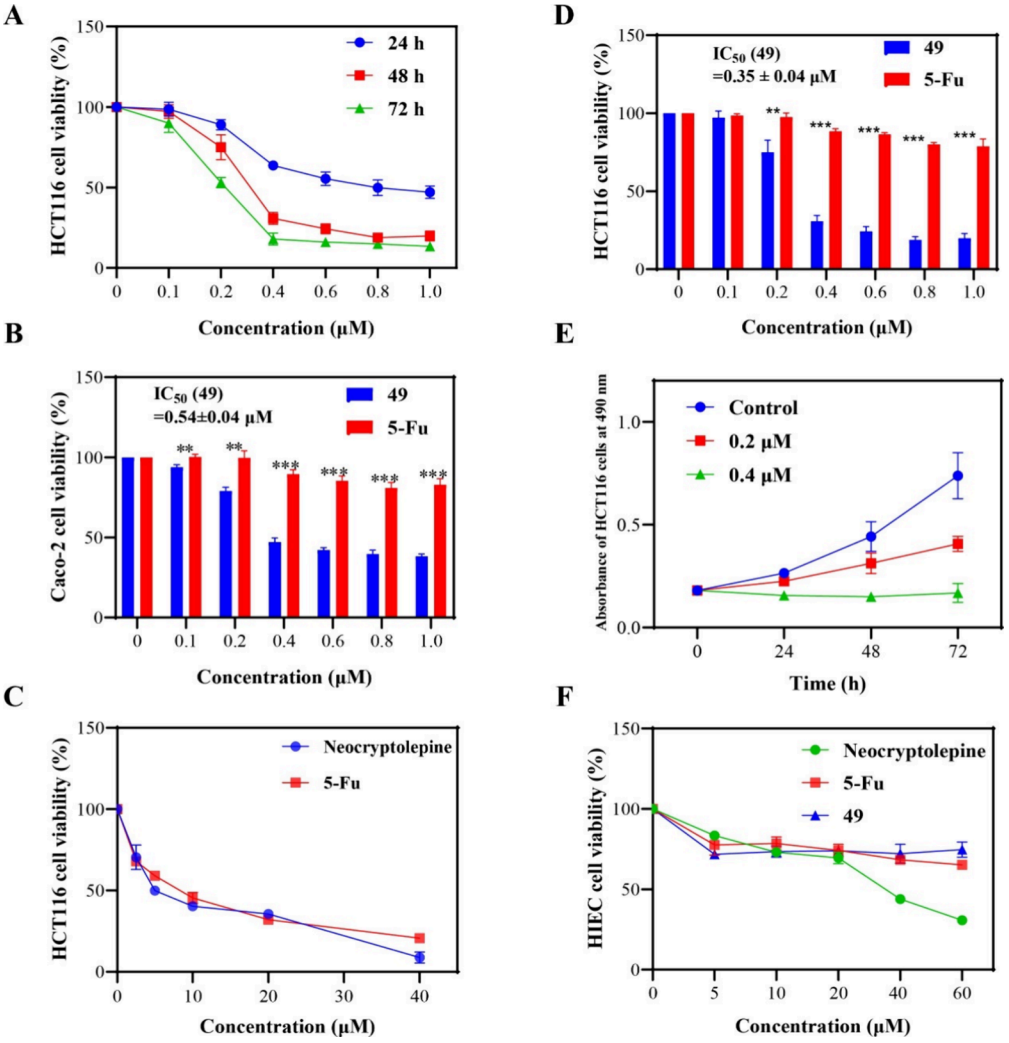


**Figure 1.** Effects of compound **49** on HCT116 and Caco-2 cells. (A) Concentration and time-dependent effects of compound **49** on HCT116 cells. (B–D) Compound **49** had a better anticancer activity than 5-Fu on HCT116 and Caco-2 cells. (E) The $OD_{490\ nm}$ values of cells treated with compound **49** in HCT116 cell lines. Values were shown as the mean ± SD, $n = 3$. *$p$ <0.05, **$p$ <0.01, ***$p$ <0.001.

cytotoxicity on HCT116 cells at the same concentration (Figure 1D). Moreover, The $IC_{50}$ of compound **49** in human normal intestinal epithelial HIEC cells was greater than 50 $\mu$M (Figure 1F). Therefore, compared with neocryptolepine, the introduction of 2-site Cl atom and 8-site methoxyl substituents made the cytotoxicity of compound **49** better in colorectal cancer cells. The 2-site Cl and 8-site methoxyl could be important substituents for compound **49** to exert good cytotoxic effects. Taken together, compound **49** displayed excellent cytotoxic activity to CRC cells and low toxicity to normal intestinal epithelial cells.

**3.3. Compound 49 Inhibited the Plate Clone Formation of Colorectal Cells and Blocked the Colorectal Cell Cycle at the G2/M Stage.** To further verify the cytotoxicity of compound **49** *in vitro*, plate clone formation assay was performed. According to Figure 2A,B, compound **49** inhibited the formation of HCT116 and Caco-2 cell clones. These results suggested that compound **49** could inhibit the proliferation of HCT116 and Caco-2 cells. Anticancer drugs of small molecules often interfere with the cancer cell cycle.[30] It has been reported that neocryptolepine intercalated into DNA and interfered with the catalytic activity of human topoisomerase II, provoked a massive accumulation of P388 murine leukemia cells at the G2/M phase.[31] To determine the mechanisms by which compound **49** exerted cytotoxicity, HCT116 and Caco-2 cell cycle distribution was examined by flow cytometry. According to Figure 2C,D, the HCT116 and Caco-2 cell cycle progression was significantly arrested at the G2/M phase in a concentration-dependent manner. The percentage of the G2/M phase HCT116 and Caco-2 cells increased from 15.21 to 82.53% and from 23.22 to 86.48% after the treatment of compound **49** at different concentrations (0, 0.2, and 0.4 $\mu$M) for 24 h (Table 2). These results suggested that compound **49** could induce cell cycle arrest at the G2/M phase.

**3.4. Compound 49 Inhibited the Migration of Colorectal Cells.** Cell migration is critical in cancer invasion and progression,[32] and metastases have been the major cause of cancer-associated deaths in general.[33] The transwell assay was performed to investigate the effect of compound **49** on HCT116 cell migration. According to Figure 4B, after treatment of compound **49**, the number of migratory cells of HCT116 was significantly reduced in a dose-dependent manner. The results suggested that compound **49** inhibited the migration of HCT116 cells.



https://doi.org/10.1021/acsomega.4c03101
ACS Omega 2024, 9, 30698−30707

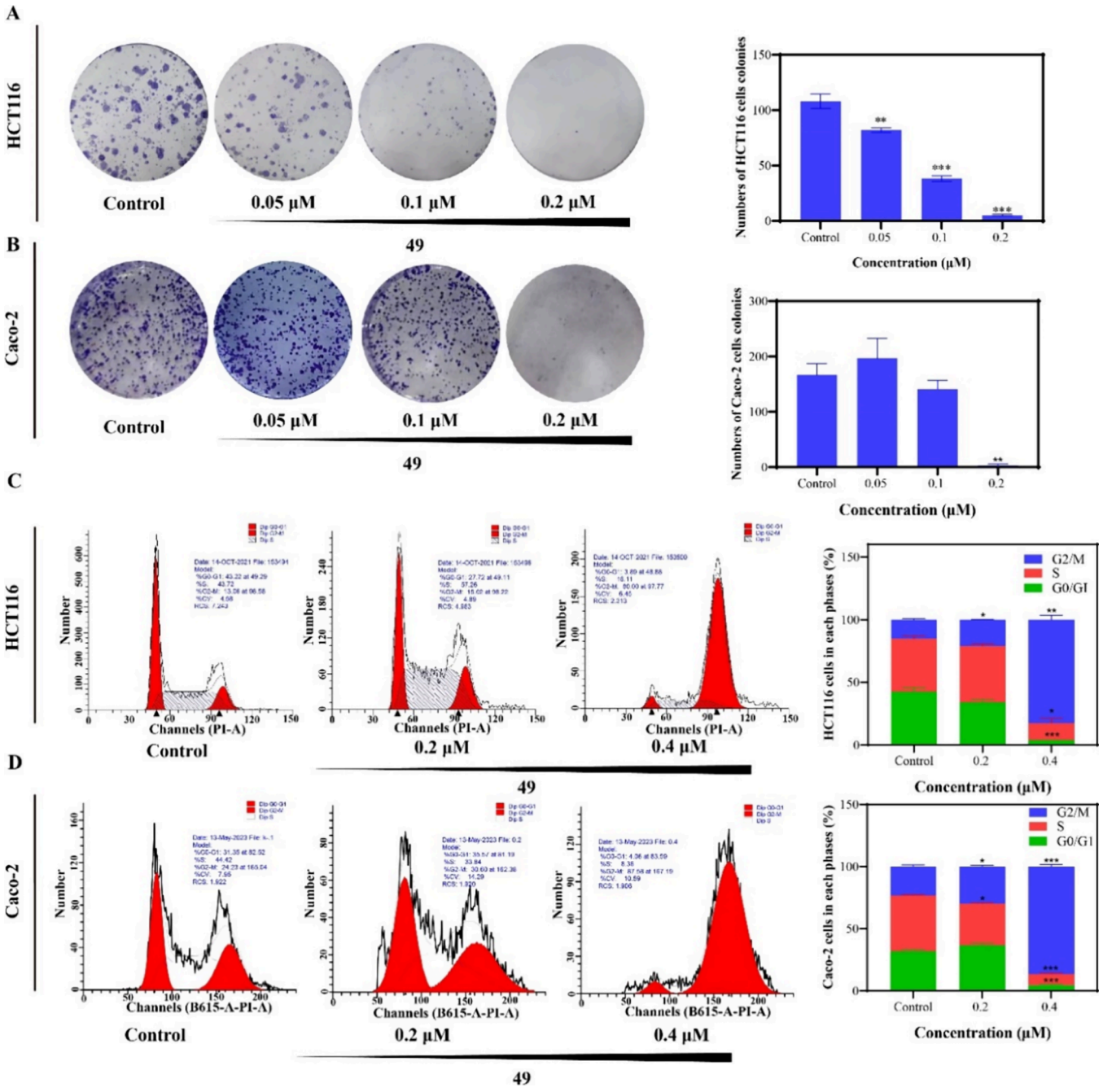


**Figure 2.** Effect of compound **49** on HCT116 cell colony formation and cell cycle. (A) Compound **49** inhibited colony formation of HCT116 cells. (B) Compound **49** inhibited colony formation of Caco-2 cells. (C) HCT116 cells were treated with compound **49** (0, 0.2, and 0.4 $\mu$M) for 24 h and analyzed by flowed cytometry. (D) Caco-2 cells were treated with compound **49** (0, 0.2, and 0.4 $\mu$M) for 24 h and analyzed by flowed cytometry. Values were shown as the means ± SD, $n$ = 3, *$p$ <0.05, **$p$ <0.01, ***$p$ <0.001.

**Table 2. Effects of Compound 49 on the Cell Cycle Distribution of HCT116 and Caco-2 Cells Treated for 24 h**

| | the distribution of HCT116 cells in each phase (%) | | | the distribution of Caco-2 cells in each phase (%) | | |
|---|---|---|---|---|---|---|
| compound **49** | G0/G1 | *S* | G2/M | G0/G1 | *S* | G2/M |
| control | 42.56 ± 3.31 | 42.23 ± 2.37 | 15.21 ± 0.94 | 32.04 ± 0.97 | 44.75 ± 0.47 | 23.22 ± 1.44 |
| 0.2 $\mu$M | 34.12 ± 2.20 | 44.88 ± 2.00 | 21.01 ± 0.20 | 36.68 ± 1.57 | 33.52 ± 0.45 | 29.81 ± 1.12 |
| 0.4 $\mu$M | 3.92 ± 0.04 | 13.55 ± 3.61 | 82.53 ± 3.56 | 4.54 ± 0.67 | 8.99 ± 0.89 | 86.48 ± 1.56 |

**3.5. Compound 49 Produced ROS, Disrupted MMP, and Induced Cell Apoptosis.** To determine whether compound **49** affects HCT116 apoptosis, we analyzed HCT116 cells treated by compound **49** using the qualitative approach of the Hoechst 33258 staining assay. The result showed that the number of brightly fluorescent cells increased in a concentration-dependent manner (Figure 4A). That means compound **49** could induce the apoptosis of HCT116


https://doi.org/10.1021/acsomega.4c03101
ACS Omega 2024, 9, 30698−30707

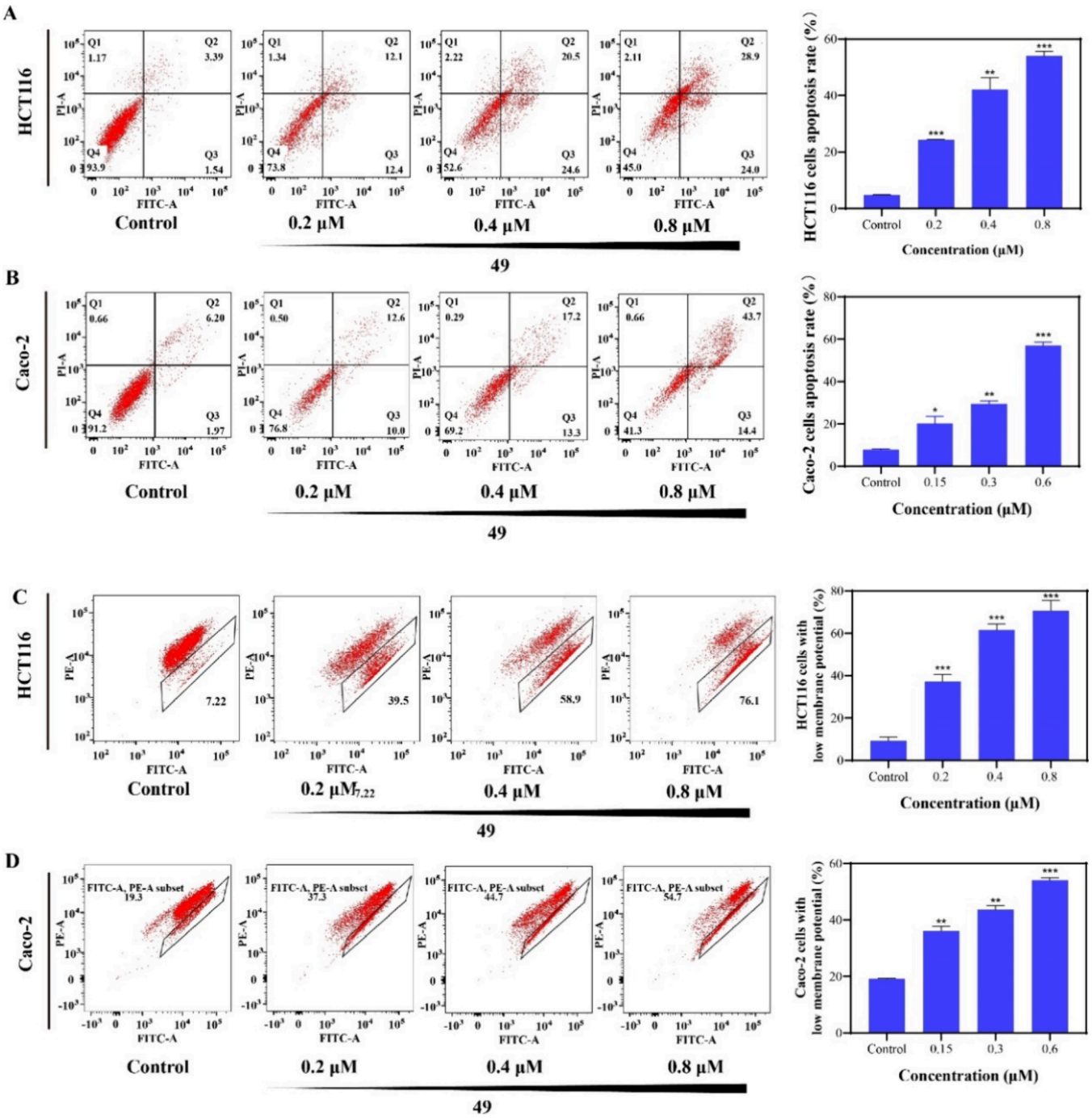


**Figure 3.** Effect of compound **49** on colorectal cell apoptosis. (A) Analysis of HCT116 cell apoptosis induced by compound **49** (0, 0.2, 0.4, and 0.8 $\mu$M) using the Annexin V/PI assay. (B) Analysis of Caco-2 cell apoptosis induced by compound **49** (0, 0.2, 0.4, and 0.8 $\mu$M) using the Annexin V/PI assay. (C, D) The depolarization of MMP in HCT116 and Caco-2 cells after treatment with compound **49** (0, 0.2, 0.4, and 0.8 $\mu$M) for 48 h by the JC-10 assay. Values were shown as the means ± SD, $n$ = 3, *$p$ <0.05, **$p$ <0.01, ***$p$ <0.001.

cells. To further quantitatively test the effect of compound **49** on apoptosis of HCT116 cells, an Annexin V-Alexa Fluor 488/PI staining assay was performed. As shown in Figure 3A,B, compound **49** mainly caused late apoptosis; the percentage of late apoptotic HCT116 cells increased from 3.7 to 45.3%, and the percentage of late apoptotic Caco-2 cells increased from 11.6 to 43.0%. The percentage of early and late stages apoptotic cells increased from 4.89 to 54.00% in HCT116 cells and from 7.86 to 71.50% in Caco-2 cells after the treatment of compound **49** at different concentrations (0, 0.2, 0.4, and 0.8 $\mu$M) for 48 h, which suggested that compound **49** significantly increased the cellular apoptosis in a concentration-dependent manner (Table 3).

Early apoptosis is often accompanied by the reduction of the mitochondrial membrane potential, so we performed JC-10 staining experiments to detect the effect of compound **49** on the mitochondrial membrane potential of HCT116 and Caco-2 cells. According to Figure 3C,D, HCT116 cells with reduced mitochondrial membrane potential increased from 7.2 to 76.1%, and Caco-2 cells with reduced mitochondrial


https://doi.org/10.1021/acsomega.4c03101
ACS Omega 2024, 9, 30698−30707

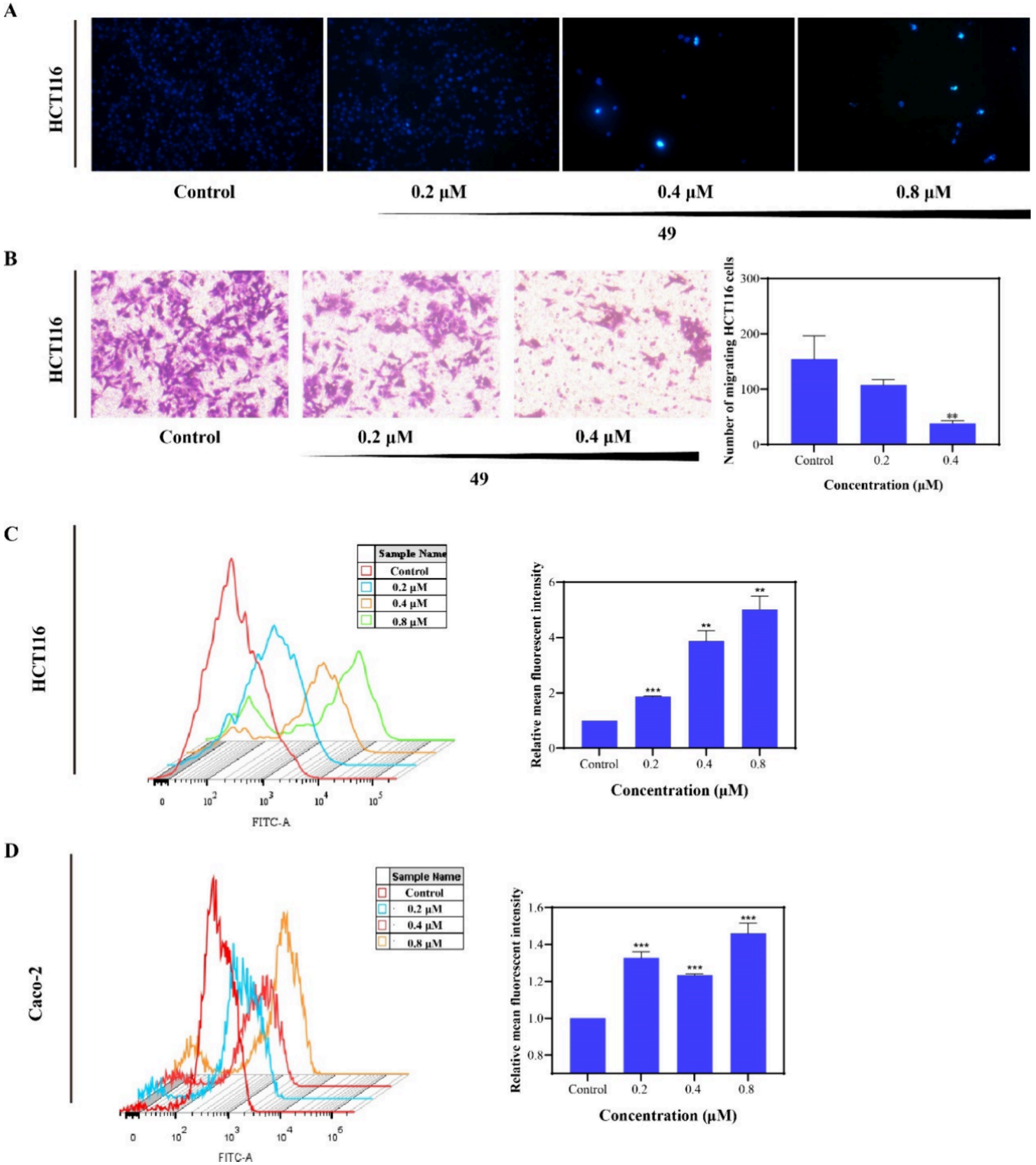


**Figure 4.** Compound **49** induced early apoptosis and inhibited cell migration of HCT116 and increased the ROS level of HCT116 and Caco-2 cells. (A) Compound **49** induced early apoptosis of HCT116. (B) Compound **49** inhibited cell migration of HCT116 cells. (C, D) Analysis of ROS induced by compound **49** (0, 0.2, 0.4, and 0.8 $\mu$M) for 48 h using the DCFH-DA assay.

membrane potential increased from 19.2 to 54.0%. These results indicated that compound **49** could significantly cause a reduction in mitochondrial membrane potential in HCT116 and Caco-2 cells.

The production of ROS can affect the integrity of mitochondrial membranes, which is the basis of maintaining a normal level of mitochondrial membrane potential. To verify whether ROS was involved in the decrease in mitochondrial membrane potential, changes in ROS production were detected in HCT116 and Caco-2 cells treated with different concentrations (0, 0.2, 0.4, and 0.8 $\mu$M) of compound **49** for 48 h. As shown in Figure 4C,D, the relative fluorescence



https://doi.org/10.1021/acsomega.4c03101
ACS Omega 2024, 9, 30698−30707

**Table 3. Apoptosis Rate of HCT116 and Caco-2 Cells Treated with Compound 49 for 48 h**

| compound 49 | the apoptosis rate of HCT116 cells (%) | the apoptosis rate of Caco-2 cells (%) |
|---|---|---|
| control | 4.89 ± 0.06 | 7.86 ± 0.44 |
| 0.2 $\mu$M | 24.35 ± 0.21 | 35.05 ± 4.03 |
| 0.4 $\mu$M | 42.20 ± 4.10 | 50.40 ± 1.84 |
| 0.8 $\mu$M | 54.00 ± 1.56 | 71.50 ± 2.83 |

intensity of DCF of HCT116 cells increased from 1.00 to 5.02 and the relative fluorescence intensity of DCF of Caco-2 cells increased from 1.00 to 1.46 after treatment with compound **49** (Table 4).

**Table 4. Relative Mean Fluorescent Intensity of HCT116 and Caco-2 Cells Treated with Compound 49 for 48 h**

| compound 49 | the relative mean fluorescent intensity of HCT116 cells | the relative mean fluorescent intensity of Caco-2 cells |
|---|---|---|
| control | 1.00 ± 0.00 | 1.00 ± 0.00 |
| 0.2 $\mu$M | 1.87 ± 0.03 | 1.33 ± 0.03 |
| 0.4 $\mu$M | 3.87 ± 0.38 | 1.23 ± 0.01 |
| 0.8 $\mu$M | 5.02 ± 0.49 | 1.46 ± 0.05 |

These results indicated a significant and concentration-dependent increase in cellular ROS production after the treatment of compound **49**. Subsequently, the mitochondrial apoptosis pathway was verified by examining the expression of related proteins. According to Figure 5B, the expression level of cleaved-caspase 9 protein was significantly upregulated after treatment of compound **49** for 48 h. In conclusion, compound **49** might induce the apoptosis of HCT116 and Caco-2 cells by activating the mitochondrial pathway.

**3.6. Compound 49 Regulated the PI3K/AKT/mTOR Signaling Pathway in Colorectal Cancer HCT116 and Caco-2 Cells.** As shown in Figure 5A, molecular docking results supported the possibility that PI3KCA was the target of the action of compound **49**. The positively charged amino group on lysine 802 formed a stable hydrogen bond interaction with the oxygen atom on the methoxy of the acceptor, and the phenyl ring on compound **49** formed a $\pi-\pi$ stacking interaction with tryptophan 780. Moreover, the ligand small molecule compound **49** was in a hydrophobic cavity consisting of 772MET, 850VAL, 922MET, 930PHE, 851VAL, 836TYR, 800ILE, 848ILE, 932ILE, 807LEU, and 934PHE, forming a strong hydrophobic interaction. The CDK1 plays an important role at the G2/M transition in the cell cycle, and the activity of CDK1 depends on the binding of CDK to cyclin B1. Western blot experiments were used to evaluated the protein expression

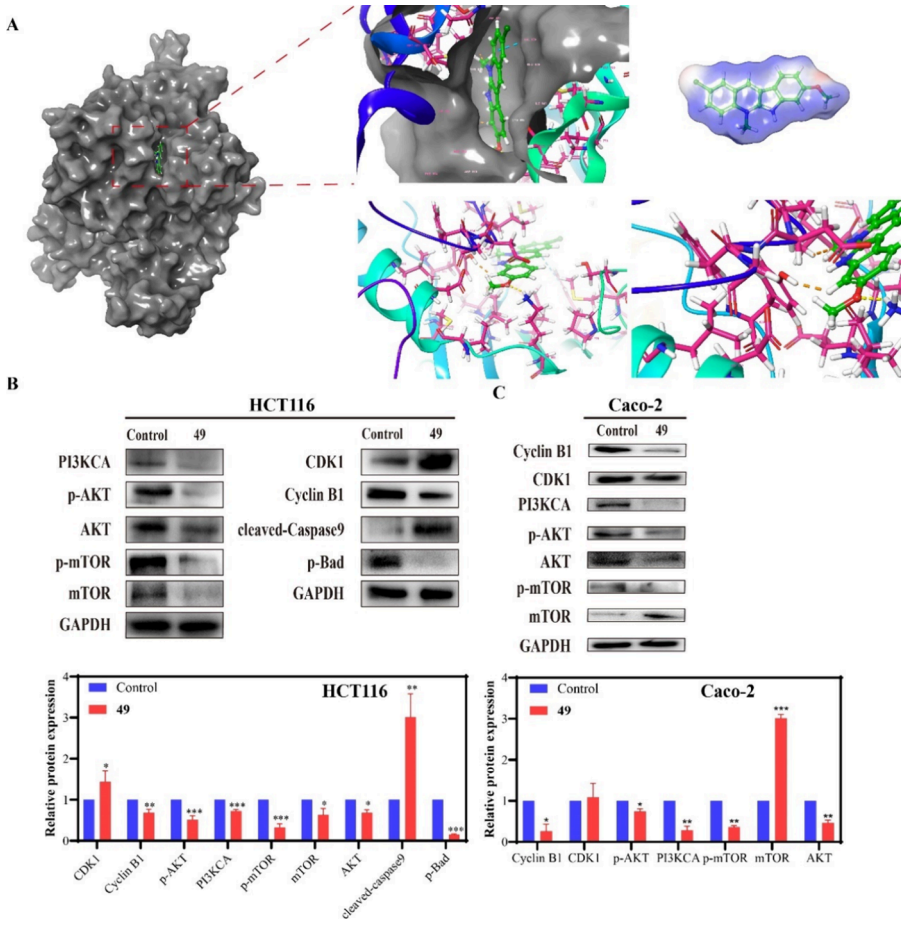


**Figure 5.** Result of molecular docking between compound **49** and PI3KCA receptor and compound **49** regulated the PI3K/Akt signaling pathway and cell cycle-related protein expression. (A) The result of molecular docking between compound **49** and the PI3KCA receptor. (B, C) The expression levels of related proteins in HCT116 and Caco-2 cells after treatment with compound **49** for 48 h. Values are shown as the means ± SD, $n = 3$, $^{*}p < 0.05$, $^{**}p < 0.01$, $^{***}p < 0.001$.



https://doi.org/10.1021/acsomega.4c03101
ACS Omega 2024, 9, 30698−30707

levels of related signaling pathways after the treatment of compound **49**. As shown in Figure 5B,C, the results revealed that the expression level of PI3KCA and p-AKT proteins was downregulated in HCT116 and Caco-2 cells after treatment of compound **49**. In addition, the expression level of the CDK1 protein was upregulated, while the expression level of the cyclin B1 protein was downregulated. These results suggested that compound **49** might induce cell apoptosis of HCT116 and Caco-2 cells by regulating the PI3K/AKT/mTOR cell signaling pathway, thereby exhibiting cytotoxic effects.

Significant changes in cellular signaling pathways occur during cancer development.[24] Numerous studies have shown that targeting signaling pathways to treat cancer is a promising strategy.[34,35] The PI3K/AKT/mTOR signaling pathway is one of the most frequently activated signaling pathways in human cancers. As multiple genes of the PI3K/AKT/mTOR signaling pathway are frequently altered in human cancers, the genes related with this pathway are important molecular therapeutic targets in cancer treatment.[25] Therefore, the regulatory role of compound **49** in this pathway was examined. In this study, MTT results showed that compound **49** could exert better cytotoxic effects on HCT116 and Caco-2 cells than the positive drug 5-Fu and have less toxicity to normal cells. Cell cloning and cell migration assays showed that compound **49** could inhibit colorectal cell proliferation and migration. Flow cytometry results indicated that compound **49** could block the cell cycle in the G2/M phase and induce cell apoptosis by the mitochondrial pathway. Molecular docking and Western blot results suggested that compound **49** might exert cytotoxicity by affecting the protein expression related PI3K/AKT/mTOR signaling pathway and cell cycle. Considering these results, compound **49** may be a promising lead compound for the treatment of colorectal cancer and provide support for subsequent structural modifications of the compounds.

## 4. CONCLUSIONS

In this study, MTT results showed that compound **49** could exert better cytotoxic effects than the positive drug 5-Fu and less toxicity to normal cells. Plate clone formation and cell migration assays showed that compound **49** could inhibit colorectal cell proliferation and migration. Flow cytometry results indicated that compound **49** could arrest the cell cycle in the G2/M phase and induce cell apoptosis by the mitochondrial pathway in HCT116 and Caco-2 cells. Molecular docking and Western blot results suggested that compound **49** might exert cytotoxicity by regulating the key protein expression related to the PI3K/AKT/mTOR signaling pathway and cell cycle. Considering these results, compound **49** might be a promising lead compound for the treatment of colorectal cancer and provide support for subsequent structural modifications of the compounds.

## ■ ASSOCIATED CONTENT

### Supporting Information

The Supporting Information is available free of charge at https://pubs.acs.org/doi/10.1021/acsomega.4c03101.

$^{1}$H and $^{13}$C NMR spectra of compound **49** and its high-resolution mass spectrogram, and the purity test of compound **49** by HPLC (PDF)

## ■ AUTHOR INFORMATION


### Corresponding Authors

**Yingqian Liu** − *School of Pharmacy, Lanzhou University, Lanzhou, Gansu 730000, China*; orcid.org/0000-0001-5040-2516; Phone: +86 931 8915686; Email: yqliu@lzu.edu.cn; Fax: +86 931 8915686

**Peng Chen** − *School of Pharmacy, Lanzhou University, Lanzhou, Gansu 730000, China*; Email: chenpeng@lzu.edu.cn

### Authors

**Yunhao Ma** − *School of Pharmacy, Lanzhou University, Lanzhou, Gansu 730000, China*

**Hongmei Zhu** − *School of Pharmacy, Lanzhou University, Lanzhou, Gansu 730000, China*

**Xinrong Jiang** − *School of Pharmacy, Lanzhou University, Lanzhou, Gansu 730000, China*

**Zhongkun Zhou** − *School of Pharmacy, Lanzhou University, Lanzhou, Gansu 730000, China*

**Yong Zhou** − *School of Pharmacy, Lanzhou University, Lanzhou, Gansu 730000, China*

**Yanan Tian** − *Faculty of Applied Sciences, Macao Polytechnic University, Macau 999078, China*

**Lixue Tu** − *School of Pharmacy, Lanzhou University, Lanzhou, Gansu 730000, China*

**Juan Lu** − *School of Pharmacy, Lanzhou University, Lanzhou, Gansu 730000, China*; orcid.org/0009-0002-5655-9068

**Yuqing Niu** − *School of Pharmacy, Lanzhou University, Lanzhou, Gansu 730000, China*

**Liqian Du** − *School of Pharmacy, Lanzhou University, Lanzhou, Gansu 730000, China*

**Zhenzhen Si** − *School of Pharmacy, Lanzhou University, Lanzhou, Gansu 730000, China*

**Hong Fang** − *School of Pharmacy, Lanzhou University, Lanzhou, Gansu 730000, China*

**Huanxiang Liu** − *Faculty of Applied Sciences, Macao Polytechnic University, Macau 999078, China*; orcid.org/0000-0002-9284-3667

Complete contact information is available at: https://pubs.acs.org/10.1021/acsomega.4c03101


### Author Contributions

[§]Y.M. and H.Z. contributed equally to this work.

### Notes

The authors declare no competing financial interest.

## ■ ACKNOWLEDGMENTS

This work was supported by the Technological Innovation Guidance Program of Gansu Province (Grant No. 21CX6QA127), Scientific Research Project of Gansu Medical Products Administration (Grant No. 2022GSMPA008), Gansu Intellectual Property Project (Grant No. 22ZSCQ065), Technology Program of Lanzhou City (Grant No. 2022-2-52), and the College Students' Innovation and Entrepreneurship Program of Lanzhou University, China (Grant Nos. 20240260001 and 20240260017).

## ■ REFERENCES

(1) Bahrami, A.; Khazaei, M.; Hasanzadeh, M.; ShahidSales, S.; Joudi Mashhad, M.; Farazestanian, M.; Sadeghnia, H. R.; Rezayi, M.; Maftouh, M.; Hassanian, S. M.; Avan, A. Therapeutic Potential of Targeting PI3K/AKT Pathway in Treatment of Colorectal Cancer: Rational and Progress. *J. Cell Biochem* **2018**, *119* (3), 2460−2469.



https://doi.org/10.1021/acsomega.4c03101
*ACS Omega* 2024, 9, 30698−30707

(2) Kasprzak, A. Insulin-Like Growth Factor 1 (IGF-1) Signaling in Glucose Metabolism in Colorectal Cancer. *Int. J. Mol. Sci.* **2021**, *22* (12), 6434.
(3) Cao, W.; Chen, H.-D.; Yu, Y.-W.; Li, N.; Chen, W.-Q. Changing profiles of cancer burden worldwide and in China: a secondary analysis of the global cancer statistics 2020. *Chin Med. J. (Engl)* **2021**, *134* (7), 783−791.
(4) Sung, H.; Ferlay, J.; Siegel, R. L.; Laversanne, M.; Soerjomataram, I.; Jemal, A.; Bray, F. Global Cancer Statistics 2020: GLOBOCAN Estimates of Incidence and Mortality Worldwide for 36 Cancers in 185 Countries. *CA Cancer J. Clin* **2021**, *71* (3), 209−249.
(5) Hu, S. J.; Ma, W.; Wang, J.; Zhou, Z.; Ma, Y.; Zhang, R.; Du, K.; Zhang, H.; Sun, M.; Jiang, X.; Tu, H.; Tang, X.; Yao, X.; Chen, P. Synthesis and biological activity of 1H-imidazo[4,5-f][1,10]-phenanthroline as a potential antitumor agent with PI3K/AKT/mTOR signaling. *Eur. J. Pharmacol.* **2022**, *915*, No. 174514.
(6) Karpisheh, V.; Joshi, N.; Zekiy, A. O.; Beyzai, B.; Hojjat-Farsangi, M.; Namdar, A.; Edalati, M.; Jadidi-Niaragh, F. EP4 receptor as a novel promising therapeutic target in colon cancer. *Pathol Res. Pract* **2020**, *216* (12), No. 153247.
(7) Messersmith, W. A. NCCN Guidelines Updates: Management of Metastatic Colorectal Cancer. *J. Natl. Compr. Cancer Network* **2019**, *17* (5.5), 599−601.
(8) Chen, P.; Xu, R.; Wang, J.; Wu, Z.; Yan, L.; Zhao, W.; Liu, Y.; Ma, W.; Shi, X.; Li, H. Starch biotransformation into isomaltooligosaccharides using thermostable alpha-glucosidase from Geobacillus stearothermophilus. *PeerJ.* **2018**, *6*, No. e5086.
(9) McQuade, R. M.; Stojanovska, V.; Bornstein, J. C.; Nurgali, K. Colorectal Cancer Chemotherapy: The Evolution of Treatment and New Approaches. *Curr. Med. Chem.* **2017**, *24* (15), 1537−1557.
(10) Guo, J.; Yu, Z.; Das, M.; Huang, L. Nano Codelivery of Oxaliplatin and Folinic Acid Achieves Synergistic Chemo-Immunotherapy with 5-Fluorouracil for Colorectal Cancer and Liver Metastasis. *ACS Nano* **2020**, *14* (4), 5075−5089.
(11) Rejhová, A.; Opattová, A.; Čumová, A.; Slíva, D.; Vodička, P. Natural compounds and combination therapy in colorectal cancer treatment. *Eur. J. Med. Chem.* **2018**, *144*, 582−594.
(12) Wan, Y.; Long, J.; Gao, H.; Tang, Z. 2-Aminothiazole: A privileged scaffold for the discovery of anti-cancer agents. *Eur. J. Med. Chem.* **2021**, *210*, No. 112953.
(13) Tuyiringire, N.; Deyno, S.; Weisheit, A.; Tolo, C. U.; Tusubira, D.; Munyampundu, J.-P.; Ogwang, P. E.; Muvunyi, C. M.; Heyden, Y. V. Three promising antimycobacterial medicinal plants reviewed as potential sources of drug hit candidates against multidrug-resistant tuberculosis. *Tuberculosis (Edinb)* **2020**, *124*, No. 101987.
(14) Hua, F.; Shang, S.; Hu, Z.-W. Seeking new anti-cancer agents from autophagy-regulating natural products. *J. Asian Nat. Prod Res.* **2017**, *19* (4), 305−313.
(15) Brito, L. D. C.; Berenger, A. L. R.; Figueiredo, M. R. An overview of anticancer activity of Garcinia and Hypericum. *Food Chem. Toxicol.* **2017**, *109* (2), 847−862.
(16) Maffioli, S. I.; Cruz, J. C. S.; Monciardini, P.; Sosio, M.; Donadio, S. Advancing cell wall inhibitors towards clinical applications. *J. Ind. Microbiol Biotechnol* **2016**, *43* (2−3), 177−184.
(17) Rudolf, G. C.; Koch, M. F.; Mandl, F. A. M.; Sieber, S. A. Subclass-specific labeling of protein-reactive natural products with customized nucleophilic probes. *Chemistry* **2015**, *21* (9), 3701−3707.
(18) Yan, Y.; Li, X.; Zhang, C.; Lv, L.; Gao, B.; Li, M. Research Progress on Antibacterial Activities and Mechanisms of Natural Alkaloids: A Review. *Antibiotics (Basel)* **2021**, *10* (3), 318.
(19) Shnyder, S. D.; Wright, C. W. Recent Advances in the Chemistry and Pharmacology of Cryptolepine. *Prog. Chem. Org. Nat. Prod* **2021**, *115*, 177−203.
(20) Zhu, J. K.; Gao, J. M.; Yang, C. J.; Shang, X. F.; Zhao, Z. M.; Lawoe, R. K.; Zhou, R.; Sun, Y.; Yin, X. D.; Liu, Y. Q. Design, Synthesis, and Antifungal Evaluation of Neocryptolepine Derivatives against Phytopathogenic Fungi. *J. Agric. Food. Chem.* **2020**, *68* (8), 2306−2315.
(21) Larghi, E. L.; Bracca, A. B. J.; Arroyo Aguilar, A. A.; Heredia, D. A.; Pergomet, J. L.; Simonetti, S. O.; Kaufman, T. S. Neocryptolepine: A Promising Indoloisoquinoline Alkaloid with Interesting Biological Activity. Evaluation of the Drug and its Most Relevant Analogs. *Curr. Top Med. Chem.* **2015**, *15* (17), 1683−1707.
(22) Zhou, S.; Huang, G. Preparation, structure and activity of polysaccharide phosphate esters. *Biomed Pharmacother* **2021**, *144*, No. 112332.
(23) Xiao, D.; Liu, Z.; Zhang, S.; Zhou, M.; He, F.; Zou, M.; Peng, J.; Xie, X.; Liu, Y.; Peng, D. Berberine Derivatives with Different Pharmacological Activities via Structural Modifications. *Mini Rev. Med. Chem.* **2018**, *18* (17), 1424−1441.
(24) Vaghari-Tabari, M.; Ferns, G. A.; Qujeq, D.; Andevari, A. N.; Sabahi, Z.; Moein, S. Signaling, metabolism, and cancer: An important relationship for therapeutic intervention. *J. Cell Physiol* **2021**, *236* (8), 5512−5532.
(25) Alzahrani, A. S. PI3K/Akt/mTOR inhibitors in cancer: At the bench and bedside. *Semin Cancer Biol.* **2019**, *59*, 125−132.
(26) Fattahi, S.; Amjadi-Moheb, F.; Tabaripour, R.; Ashrafi, G. H.; Akhavan-Niaki, H. PI3K/AKT/mTOR signaling in gastric cancer: Epigenetics and beyond. *Life Sci.* **2020**, *262*, No. 118513.
(27) He, Y.; Sun, M. M.; Zhang, G. G.; Yang, J.; Chen, K. S.; Xu, W. W.; Li, B. Targeting PI3K/Akt signal transduction for cancer therapy. *Signal Transduction Targeted Ther.* **2021**, *6* (1), 425.
(28) Yang, J.; Nie, J.; Ma, X.; Wei, Y.; Peng, Y.; Wei, X. Targeting PI3K in cancer: mechanisms and advances in clinical trials. *Mol. Cancer* **2019**, *18* (1), 26.
(29) Vecchione, M. K.; Sun, A. X.; Seidel, D. Divergent reactions of indoles with aminobenzaldehydes: indole ring-opening vs. annulation and facile synthesis of neocryptolepine. *Chemical Science* **2011**, *2* (11), 2178−2181.
(30) Uhl, E.; Wolff, F.; Mangal, S.; Dube, H.; Zanin, E. Light-Controlled Cell-Cycle Arrest and Apoptosis. *Angew. Chem., Int. Ed. Engl.* **2021**, *60* (3), 1187−1196.
(31) Dassonneville, L.; Lansiaux, A.; Wattelet, A.; Wattez, N.; Mahieu, C.; Van Miert, S.; Pieters, L.; Bailly, C. Cytotoxicity and cell cycle effects of the plant alkaloids cryptolepine and neocryptolepine: relation to drug-induced apoptosis. *Eur. J. Pharmacol.* **2000**, *409* (1), 9−18.
(32) Barriga, E. H.; Franze, K.; Charras, G.; Mayor, R. Tissue stiffening coordinates morphogenesis by triggering collective cell migration in vivo. *Nature* **2018**, *554* (7693), 523−527.
(33) Weiße, J.; Rosemann, J.; Krauspe, V.; Kappler, M.; Eckert, A. W.; Haemmerle, M.; Gutschner, T. RNA-Binding Proteins as Regulators of Migration, Invasion and Metastasis in Oral Squamous Cell Carcinoma. *Int. J. Mol. Sci.* **2020**, *21* (18), 6835.
(34) Asati, V.; Mahapatra, D. K.; Bharti, S. K. PI3K/Akt/mTOR and Ras/Raf/MEK/ERK signaling pathways inhibitors as anticancer agents: Structural and pharmacological perspectives. *Eur. J. Med. Chem.* **2016**, *109*, 314−341.
(35) Zou, S.; Tong, Q.; Liu, B.; Huang, W.; Tian, Y.; Fu, X. Targeting STAT3 in Cancer Immunotherapy. *Mol. Cancer* **2020**, *19* (1), 145.


https://doi.org/10.1021/acsomega.4c03101
*ACS Omega* 2024, 9, 30698−30707